It is felt by the authors that actual flight hardware development based on the results of the work presented in this note could be simple and reliable. Scaled down versions of the system discussed could be suspended over the surfaces which display the more serious outgassing problem. Each of these small jets could be mounted so that it could sweep across the window surfaces. In this manner a small jet could be used to clean a large area, by cleaning one area, then moving to another. However, the principal purpose of this effort was to establish a feasible method of removing contaminants similar to those encountered and little effort was expended on development of optimum hardware.

Quasi-Steady Solution for Ablation-Erosion Heat Transfer

Victor Quan*
TRW Systems, Redondo Beach, Calif.

The quasi-steady temperature distribution and surface recession rate ($\dot{S}$) for a material undergoing internal decomposition and surface ablation and erosion are rapidly approached when a vehicle travels at hypersonic speeds and when the rate ($\dot{S}$) is high. By "quasi-steady state" we mean that changes in the temperature distribution in the material, as measured from the moving surface, are small with respect to time. Erosion here refers to material removal due to chemical reaction, aerodynamic force, and particle impact (if a vehicle enters a rain, ice, or dust environment); whereas ablation refers to phase change such as sublimation. The erosion rate, heat rate, and surface temperature are interdependent and hence must be calculated simultaneously. Erosion thus differs from ablation which occurs at a unique known surface temperature. The present analysis treats erosion alone and combined erosion/ablation.

The solution presented not only allows for rapid estimation for engineering purposes, but it also provides a means to verify computer solutions that include a transient period. In fact, it is shown in this Note that ordinary numerical methods using finite-difference techniques to solve problems of this type are subject to two severe limitations on the maximum size of the space interval.

Heat-Transfer Model

The one-dimensional heat-transfer equation for a material that undergoes internal decomposition, or charring, is well known[1] and can be written in the form

$$\frac{\partial}{\partial t}(\rho h) = \frac{\partial}{\partial x}\left(k\frac{\partial T}{\partial x}\right) + \frac{\partial}{\partial x}\left[W(H_c + h_g)\right] \tag{1}$$

where ρ is the density of the material, h the specific enthalpy, k the thermal conductivity, W the gas flux due to decomposition, H_c the heat of decomposition, and h_g the specific enthalpy of the gas. The temperature T is a function of distance x and time t.

The density is given by

$$\rho = \rho_1 + \rho_2 \tag{2}$$

where subscript 1 refers to the decomposable resin and 2 to the char matrix. It is assumed that the density of the gas is negligible, ρ_2 is constant, and ρ_1 varies in accordance with a nth-order decomposition law,

$$\partial\rho_1/\partial t = -\rho_1{}^n A \exp(-B/T) \tag{3}$$

where n, A, and B are empirical constants.

The enthalpy is taken as

$$\rho h = (\rho_1 c_1 + \rho_2 c_2)T \tag{4}$$

where the specific heats c_1 and c_2 are assumed constant. The conductivity is assumed to follow a linear relation of the form

$$k = C\rho_1 + D \tag{5}$$

where $C = (k_\infty - k_2)/\rho_{1\infty}$, and $D = k_2$ are constants, and the subscript ∞ referring to virgin state.

The gas flux is related to ρ_1 by the continuity equation of

$$\partial W/\partial x = \partial\rho_1/\partial t \tag{6}$$

Assuming the gas to be in thermal equilibrium with the solid and to have a constant specific heat c_g, one may write

$$h_g = c_g T \tag{7}$$

Equations (1–7) completely define the mathematical model for heat transfer in a charring material. The quasi-steady analysis and the boundary conditions involving a receding surface are given in the next section.

Analysis for Quasi-Steady State

By introducing the transformation of

$$z = x - S \tag{8}$$

Eqs. (1, 3, and 6) become

$$\left(\frac{\partial}{\partial t}\rho h\right)_z - \dot{S}\left(\frac{\partial}{\partial z}\rho h\right)_t = \frac{\partial}{\partial z}\left[k\frac{\partial T}{\partial z} + W(H_c + h_g)\right]_t \tag{9}$$

$$(\partial\rho_1/\partial t)_z - \dot{S}(\partial\rho_1/\partial z)_t = -\rho_1{}^n A \exp(-B/T) \tag{10}$$

$$(\partial W/\partial z)_t = (\partial\rho_1/\partial t)_z - \dot{S}(\partial\rho_1/\partial z)_t \tag{11}$$

where S is the distance from $x = 0$ to the surface at time t, and $\dot{S} \equiv dS/dt$ is the surface recession rate.

In the quasi-steady analysis, it is assumed that $(\partial T/\partial t)_z$ and $(\partial\rho_1/\partial t)_z$ are negligible. This is acceptable when the heating rate Q and $\dot{S}$ are high. Physically, this implies that heat storage is negligible compared to heat conduction and convection and that the local density change is small compared to mass convection. This situation actually occurs at hypersonic flight speeds at which the heat penetration depth and $\dot{S}$ are on the orders of 0.01 in. and 0.1 in./sec, respectively. If the vehicle enters a time-dependent environment, the present solution is still applicable if one assumes the material to adjust to the present condition instantaneously. It is further assumed that $\dot{S}$ is constant over a time interval. Using the boundary conditions of $T = T_\infty$, $\rho_1 = \rho_{1\infty}$, and $W = 0$ at $z \rightarrow \infty$, Eqs. (9) and (11) can be integrated to yield

$$(C\rho_1 + D)(dT/dz) + W(H_c + c_g T) + \dot{S}[(\rho_1 c_1 + \rho_2 c_2)T - (\rho_{1\infty}c_1 + \rho_2 c_2)T_\infty] = 0 \tag{12}$$

$$W = \dot{S}(\rho_{1\infty} - \rho_1) \tag{13}$$

Using Eq. (13) to eliminate W, Eq. (12) becomes

$$dT/dz = -\dot{S}\zeta(T,\rho_1)/(C\rho_1 + D) \tag{14}$$

where

$$\zeta(T,\rho_1) \equiv [(\rho_{1\infty} - \rho_1)(H_c + c_g T) + (\rho_1 c_1 + \rho_2 c_2)T - (\rho_{1\infty}c_1 + \rho_2 c_2)T_\infty] \tag{15}$$

Equations (10) can be written as

$$d\rho_1/dz = (A/\dot{S})\rho_1{}^n \exp(-B/T) \tag{16}$$

Equations (14) and (16) show that $d\rho_1/dT \rightarrow \infty$ as $T \rightarrow T_\infty$,

---

Received October 24, 1969; revision received November 26, 1969.

* Member of Professional Staff, Vulnerability and Hardness Laboratory. Member AIAA.

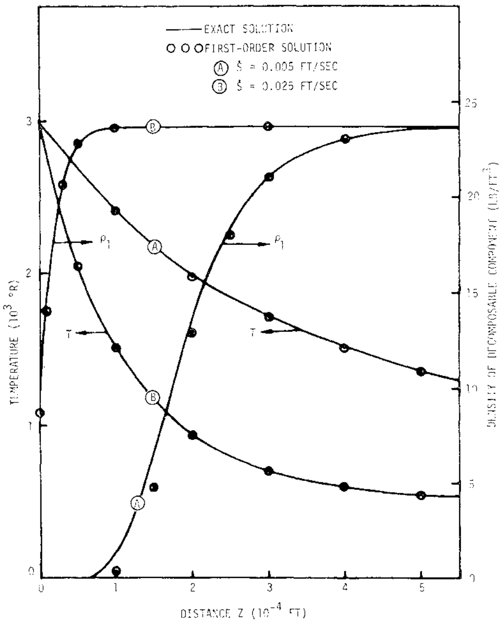

Fig. 1 Sample quasi-steady solutions for temperature and density distributions.

while in reality $d\rho_1/dT \to 0$ at low temperatures. The difficulty is due to the approximation inherent in Eq. (3) which shows $\partial\rho_1/\partial t$ to be nonzero as $x \to \infty\ (T \to T_\infty)$. To circumvent this difficulty, one may set $d\rho_1/dT = 0$ (or $\rho_1 = \rho_{1\infty}$) for $T \leq T_d$ where T_d is an arbitrary cut-off temperature below which significant amount of decomposition does not occur and T_d has a value greater than T_∞.

Equations (14) and (16) can be solved for $T(z)$ and $\rho_1(z)$ simultaneously if relations for $\dot S$ and $T(0)$ are known. These relations are obtained as follows.

Two situations can occur. First, consider the surface temperature T_0 to be below the ablation temperature T_a. Then $\dot S$ is due solely to chemical and/or mechanical erosion, and can be prescribed as a function of T_0 and density $\rho_{10} \equiv \rho_1(0)$:

$$\dot S = \dot S_e(T_0,\rho_{10}) \tag{17}$$

An example of Eq. (17) is

$$\dot S_e = K_1T_0^{K_2}e^{-K_3/T_0} + (K_4 + K_5T_0)/(\rho_{10} + \rho_2) \tag{17a}$$

where the K_i are empirical constants. In Eq. (17a), the first term on the right-hand side accounts for rate-limited chemical recession and the second term accounts for mechanical erosion by which the mass loss rate is proportional to temperature. The surface heat rate, $Q_0 \equiv -(k\partial T/\partial z)_{z=0}$ can be prescribed as a function

$$Q_0 = Q_0(\dot S_e, T_0, \rho_{10}) \tag{18}$$

An example of Eq. (18) is

$$Q_0 = h(T_c - T_0) + \sigma F(T_r^4 - T_0^4) - (\rho_{10}H_1 + \rho_2H_2)\dot S_e \tag{18a}$$

where h, T_c, σ, F, and T_r are constants denoting a heat-transfer coefficient, reference convection temperature, Stefan-Boltzmann constant, radiation shape factor, and reference radiation temperature, respectively; and H_1 and H_2 are the heats absorbed at the surface per unit mass of components 1 and 2, respectively, being eroded. It is observed that $-(k\partial T/\partial z)_{z=0}$ can be evaluated using Eq. (14) at $z = 0$ and the following relation is obtained

$$Q_0(\dot S_e, T_0, \rho_{10}) = \dot S_e(T_0,\rho_{10})\zeta(T_0,\rho_{10}) \tag{19}$$

Equations (14, 16, 17, and 19) determine $T(z)$, $\rho_1(z)$, $\dot S_e$, and T_0 simultaneously for $T_0 < T_a$.

The second case corresponds to the situation when $T_0 = T_a$, and

$$\dot S = \dot S_e + \dot S_a \tag{20}$$

Since T_0 is known, $\dot S_e$ can be prescribed as a function of surface density alone

$$\dot S_e = \dot S_e(\rho_{10}) \tag{21}$$

while the ablation rate $\dot S_a$ must be determined from a heat balance at the surface in the form

$$\dot S_a = [Q_0 - (-k\partial T/\partial z)_{z=0}]/(\rho_{10}L_1 + \rho_2L_2) \tag{22}$$

where L_1 and L_2 are the heats absorbed at the surface per unit mass of components 1 and 2, respectively, being ablated, and Q_0 is a heat rate that is independent of $\dot S_a$ given in the form

$$Q_0 = Q_0(\dot S_e, \rho_{10}) \tag{23}$$

Examples of Eqs. (21) and (23) are given by Eqs. (17a) and (18a), respectively. Using Eq. (14) to evaluate $-(k\partial T/\partial z)_{z=0}$, the following relation that determines $\dot S_a$ is obtained

$$\dot S_a = \frac{Q_0(\dot S_e,\rho_{10}) - \dot S_e(\rho_{10})\zeta(T_a,\rho_{10})}{\rho_{10}L_1 + \rho_2L_2 + \zeta(T_a,\rho_{10})} \tag{24}$$

Equations (14, 16, 20, 21, and 24) determine $T(z)$, $\rho_1(z)$, $\dot S$, $\dot S_e$, and $\dot S_a$ simultaneously for the case of combined ablation and erosion.

Approximate Solution

The exact solution is obtained by solving simultaneously the differential equations [Eqs. (14) and (16)] with the proper boundary conditions at the surface. However, a first-order approximate solution to the differential equations can be obtained in analytic form as follows.

Equations (14) and (16) can be written in the form

$$\rho_1 = \rho_{1\infty}\exp\left[\left(-\frac{A}{\dot S^2}\int_{T_d}^{T}\psi(T,\rho_1)\,e^{-B/T}\,dT\right)\right],\ n = 1 \tag{25}$$

$$\rho_1^{1-n} = \rho_{1\infty}^{1-n} + (n-1)\frac{A}{\dot S^2}\int_{T_d}^{T}\psi(T,\rho_1)\,e^{-B/T}dT,\ n \neq 1$$

$$\rho_1 = \rho_{1\infty} \text{ if } T < T_d$$

and

$$z = -\frac{1}{\dot S}\int_{T_0}^{T}\psi(T,\rho_1)dT \tag{26}$$

where

$$\psi(T,\rho_1) \equiv (C\rho_1 + D)/\zeta(T,\rho_1) \tag{27}$$

A zeroth-order solution is obtained by taking $\rho_1 = \rho_{1\infty}$. Then Eq. (26) yields the zeroth-order temperature distribution of

$$T = T_\infty + (T_0 - T_\infty)\,e^{-\phi z} \tag{28}$$

where $\phi = (\rho_{1\infty}c_1 + \rho_2c_2)\dot S/k_\infty$. The zeroth-order solution is the exact solution for a nondecomposing material, and the exponential temperature distribution is typically given[2] for ablation problems.

Using Eq. (28), a first-order density-temperature relation is calculated from Eq. (25) in which the integral becomes

$$\int_{T_d}^{T}\psi(T,\rho_1)\,e^{-B/T}\,dT = \frac{k_\infty}{\rho_{1\infty}c_1 + \rho_2c_2}\int_{T}^{T}\frac{e^{-B/T}}{T - T_\infty}\,dT \tag{29}$$

Equations (25) and (29) give the first-order $\rho_1 = \rho_1(T)$. Equations (15) and (27) become $\zeta(T,\rho_1) = \zeta(T)$ and $\psi(T,\rho_1) = \psi(T)$, respectively. Then Eq. (26) yields the first-order temperature distribution of

$$z = -\frac{1}{\dot{S}}\int_{T_0}^{T} \psi(T)dT \tag{30}$$

where T_0 is determined from Eq. (19) for erosion alone, and $T_0 = T_a$ for combined erosion and ablation.

To obtain higher-order approximations, an iterative procedure may be set up by using the first-order temperature to obtain a second-order density which in turn is used to obtain a second-order temperature, etc. However, such a procedure is more tedious than solving Eqs. (14) and (16) directly. Furthermore, the first-order solution is in general sufficiently accurate for engineering purposes. A comparison of the first-order solution and the exact solution is shown in Fig. 1 for a sample problem. It is seen that the two solutions yield nearly identical results. The figure also shows that higher erosion rate results in lower heat storage and less decomposition.

Limitations for Finite-Difference Methods

It is highly desirable to examine the limitations and magnitudes of error in employing finite-difference techniques to solve heat transfer problems with high surface recession rate. Consider the case of a noncharring material. Then the exact solution is given by Eq. (28) which, for $T_\infty = 0$, becomes

$$T/T_0 = e^{-\phi z} \tag{31}$$

where $\phi = \dot{S}/\alpha$ with α being the thermal diffusivity of the material.

A second-order finite-difference equation for quasi-steady state and constant properties can be given in the form[3]

$$(U_{i+2} - 2U_{i+1} + U_i)/h^2 + \phi[(U_{i+2} - U_i)/2h] = 0 \tag{32}$$

where U denotes a temperature obtained by finite-difference method, h is a space interval (Δz), and $i = z/h$. Equation (32) can be reduced to

$$U_{i+1} = [(1 - \phi h/2)/(1 + \phi h/2)]U_i \tag{33}$$

The solution is obviously unacceptable if $h \geq 2/\phi$. Comparison of Eq. (33) with the exact solution given by Eq. (31) shows the accumulated relative error at z (node i) to be

$$E_i \equiv \left|\frac{U_i}{T_i} - 1\right| = \left|\frac{U_0}{T_0}\left(\frac{1 - \phi h/2}{1 + \phi h/2}\right)^i e^{i\phi h} - 1\right| \tag{34}$$

The error increases monotonically with ϕh for all i. For example, even with $U_0 = T_0$, an error of 50% is developed after one step and it increases to 75% after two steps if $h > 1.65\ \alpha/\dot{S}$. It is important to note that this conclusion holds regardless of the heat flux.

Another limitation on the size of h is due to the starting value of U_0/T_0. To assess this error, let the boundary condition for unknown surface temperature be represented by a second-order numerical expression of the form

$$(3U_0 - 4U_1 + U_2)/2h = Q_s/k \tag{35}$$

where Q_s denotes the conduction heat flux at the surface. Eliminating U_1 and U_2 by using Eq. (33) and deducing $T_0 = Q_s/k\phi$ from Eq. (31), one obtains

$$E_0 = \left|\frac{U_0}{T_0} - 1\right| = \frac{\phi^2 h^2}{4(1 + \phi h)} \tag{36}$$

The magnitude of error in surface temperature is

$$|U_0 - T_0| = Q_s E_0/k\phi \tag{37}$$

Thus, while the relative error depends on ϕh only, the absolute error depends on $Q_s/k\phi$ and ϕh. The errors are given by Eqs. (34, 36, and 37). It should be pointed out that in the transient period, the errors will be greater than those indicated.

References

[1] Munson, T. R. and Spindler, R. J., "Transient Thermal Behavior of Decomposing Materials, Pt. I: General Theory and Application to Convective Heating," IAS Paper 62-30, presented at the IAS 30th Annual Meeting, New York, Jan. 22–24, 1962.

[2] Rohsenow, W. M. and Choi, H. Y., *Heat, Mass, and Momentum Transfer*, Prentice-Hall, Englewood Cliffs, N. J., 1961, pp. 122–124.

[3] Carslaw, H. S. and Jaeger, J. C., *Conduction of Heat in Solids*, 2nd ed., Oxford, 1959, Chapt. XVIII.

Attitude Control of a Sun-Pointing Spinning Spacecraft by Means of Solar Radiation Pressure

M. Chandler Crocker II*
American Science and Engineering Inc.,
Cambridge, Mass.

Nomenclature

α_1,α_2 = solar absorptivities, of sides 1 and 2 main paddles
ϵ_1,ϵ_2 = thermal emissivities, sides 1 and 2 of main paddles
α_s = solar absorptivity of the spin rate regulator paddles
H = solar constant = 1400 w/m^2
v = velocity of light = 3×10^8 m/sec
A,A_s = areas of main and spin regulator paddles
t = time, sec
d,d_s = distances from the center of mass of the satellite to the centers of pressure of the main paddle and the spin regulator paddles, respectively
I = moment of inertia of the satellite
ω,ω_0 = spin rate and initial value, respectively
F_1,F_2,F_3 = forces on a paddle due to reflected sunlight and thermal emission
L_r,L_θ,L_Φ = components of torque on the satellite in spherical coordinates due to the main paddles
$L_{rs},L_{\theta s},L_{\Phi s}$ = components of torque on the satellite due to the spin regulator paddles
β = angle between plane of the spin regulator paddles and plane of the main paddles when $\gamma = 0$
γ = angle between spin regulator paddles and spin axis
θ,Φ = angular position of the spin axis on spherical coordinates with the sun along the Z axis
θ_0,Φ_0 = initial values of θ and Φ

Introduction

SEVERAL authors[1–7] have considered using radiation pressure for attitude control of nonspinning spacecraft. Ule[8] was the first to describe a spinning satellite attitude control system for orienting the spin axis of a satellite so that the spin axis was coincident with the satellite-sun line by utilizing radiation pressure. Additional work has been done on similar devices.[9–13] Howland[14] et al. have devised a device for orienting the spin axis of a satellite perpendicular to the satellite-sun line by means of radiation pressure. This Note describes a method of maintaining the spin axis of a satellite pointing toward the sun. At the same time the spin of the satellite is maintained at a constant rate. The method requires no moving parts except springs. Electronic sensors are not required and the system requires no electrical power. As such it is well suited for satellites that are to have many years of operational life. Two larger main paddles parallel to the spin axis are used for spin axis pointing (Fig. 1); they

---

Received November 24, 1969.

* Senior Systems Engineer.